Machinability of SMART Forged Materials in Intermittent Cutting

Mitsuaki Murata[1*], Makoto Hino[2], Ryoichi Kuwano[2], Syuhei Kurokawa[3]

[1] Department of Mechanical Engineering, Kyushu Sangyo University 2-1-3 Matsukadai, Higashi-ku, Fukuoka, 813-8503 Japan.
[2] Department of Mechanical System Engineering, Hiroshima Institute of Technology, 2-1-1 Miyake, Saeki-ku, Hiroshima 731-5193 Japan.
[3] Depa rtment of Mechanical Engineering, Kyushu University, 744 Motooka, Nishi-ku, Fukuoka, 819-0935 Japan.

* Corresponding author. Tel.: +81-92-673-5627; email: murata@ip.kyusan-u.ac.jp
Manuscript submitted September 11, 2017; accepted October 16, 2017.
doi: 10.17706/ijmse.2018.6.1.1-9

Abstract: The gear shafts used in automotive transmissions are manufactured by forging high-toughness structural steels such as chrome steel or chrome-molybdenum steel, heat treating them, and then shaping the gear by cutting. In the conventional manufacturing process, there is waste of energy and work time because the forging and heat treatment processes for imparting machinability are separate. We present a new forging process that successfully imparts machinability by controlling the cooling time after forging. This research investigated the cutting machinability properties of materials made by the new SMART forging process. Mainly, as the result of investigating under the intermittent cutting about the progress of the tool wear, very good results could be obtained.

Keywords: Intermittent cutting, new forging process, tool wear, thermo-electromotive force.

1. Introduction

In conventional hot forged products, it is necessary to perform heat treatment as a post process in order to impart machinability and carburizing properties after forging. If there is no heat treatment facility in a forging plant, the forged product must be cooled, transported to a heat treatment plant, and reheated. As a solution to this challenge, we devised the SMART forging process, a method that imparts machinability and carburizing properties to forged materials by using the heat during forging [1], [2]. We accomplish this by annealing and tempering the forged materials, controlling the heat after forging without having to perform heat treatment in a separate process. Therefore, this method is superior to the conventional method in terms of the energy, cost, delivery time, and CO_2 emissions required in cooling, conveying and reheating. In this study, we examine if the SMART forged material is superior to the forgings produced by the conventional method.

In previous studies, two machinability properties were identified for SMART forged materials. First, as measured in continuous cutting, the principal force component of the SMART forging material is lower than that of the carbon steel; the cutting force is large in the high cutting speed region. Second, the progress of the flank wear was studied for continuous cutting of forging materials normalized and annealed by conventional methods versus SMART forged materials. Results indicate that there were clear differences in

the progress of the flank wear at the cutting speed of V=180 m/min or more. Furthermore, it was determined that in the high speed cutting region where the cutting speed V=200 m/min or more, the progress of flank wear in material produced via the SMART forging method was more than twice as high as that of material forged via conventional methods.

The SMART forged material we manufacture is splined, gear-processed by cutting, and shipped as a final product. Both of the cutting processes are intermittent. Therefore, we investigated whether machinability results obtained via intermittent cutting are comparable to the experimental results for continuous cutting.

2. What Is the SMART Forging Process

Fig. 1 compares the forging processes using conventional forging methods versus SMART forging. In the conventional forging method, the material is heated to 1260 degrees Celsius before forging and forged. Prior to continuing with the heat treatment step, the material is cooled to normal temperature and transported to a heat treatment plant. In order to impart machinability to the forged material, annealing treatment is performed by reheating the material to up to 900 degrees Celsius, followed by final cooling.

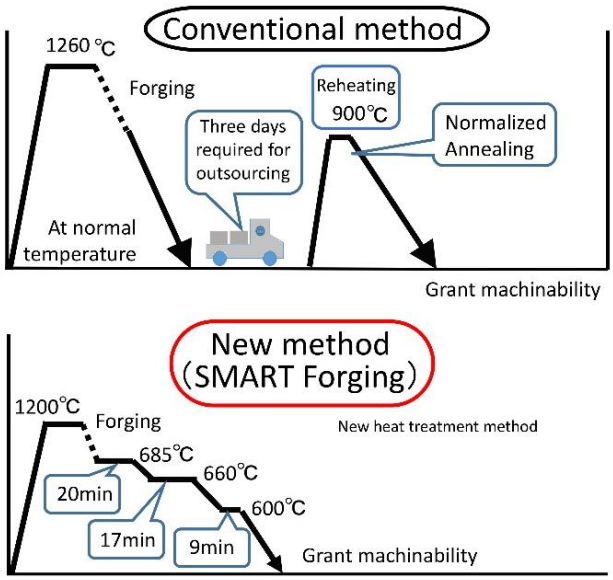

Fig. 1. Comparison between conventional forging process and the SMART forging process.

The SMART forging process starts in the same way, by heating the material up to 1200 degrees Celsius in order to perform forging. However, the SMART process cools the material while controlling the amount of heat stored in the material after forging. By following this process, it is possible to produce cutting machinability properties similar to those achieved via the conventional forging process. As a result, a superior product is produced as compared to results from conventional forging methods when considering requirements for cooling, delivery time, energy associated with reheating energy, cost and CO_2 emissions.

The machinability of materials produced via conventional forging and the SMART forging process were studied by measuring cutting forces and shearing stresses under continuous cutting process by turning. The results are shown in Fig. 2-(a) and (b). As seen in the results, the SMART forged material reflects superior properties for both the required cutting force and the shearing stresses. We note especially the difference in cutting force in the high cutting speed region of V > 200m/min.

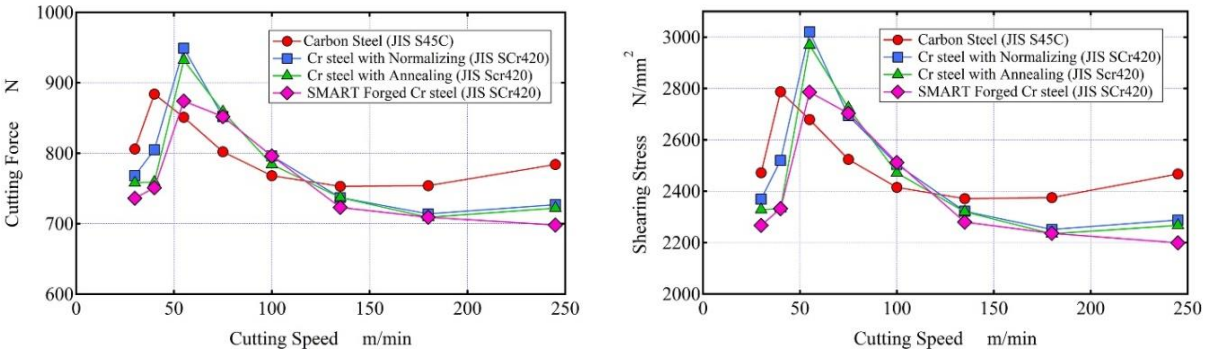

(a) Cutting force (b) Shearing stress

Fig. 2. Relationship between cutting force, shearing stress and cutting speed in continuous cutting process.

3. Experimental Method

The forged materials used in this experiment are generally shipped as parts to be used in automobile transmissions. Fig. 3 shows the forged products before the processes of gear cutting, or spline machining by cutting. These cutting process is intermittent cutting; therefore, it is necessary to compare machinability by intermittent cutting versus continuous cutting, the process used in the past. First, we compared the progress of tool flank wear during intermittent cutting by using a milling machine to compare conventionally forged materials to the SMART forged materials.

Fig. 3. SMART forged products before gear cutting process.

An illustration of the experimental apparatus is shown in Fig. 4. The face mill of diameter 100 mm was attached to the milling machine. Only one cutting edge was attached to this face mill, and the end face of the material (50mm in diameter) was cut. We intentionally did not attach more than one cutting edge because in experimental cases of abrasion, the front measured cutting edge of multiple cutting edges suffers sudden damages, and the associated influences will not affect the next edge. The rotation speed of the main spindle was determined by identifying when a clear difference in cutting force was seen in the continuous cutting experiment for cutting speeds of V=200 m/min or more. Following this approach, the experiment was conducted at cutting speeds of V=213 m/min and 308 m/min. The feed amount per cutting edge f was f=0.1 mm/edge, but this was adjusted to f=0.12 mm/edge for a cutting speed of V=213 m/min and f=0.09 mm/edge for the cutting speed of V=308 m/min in relation to the machine. The depth of cut t was set to t=1.0 mm for both cutting speeds. One cutting cycle was defined as the cutting edge cutting the end face of the workpiece once at a depth of cut t=1.0 mm. For each cycle, the tool flank face was observed with the CCD microscope shown in Fig. 4. The width of flank wear for each cycle was recorded.

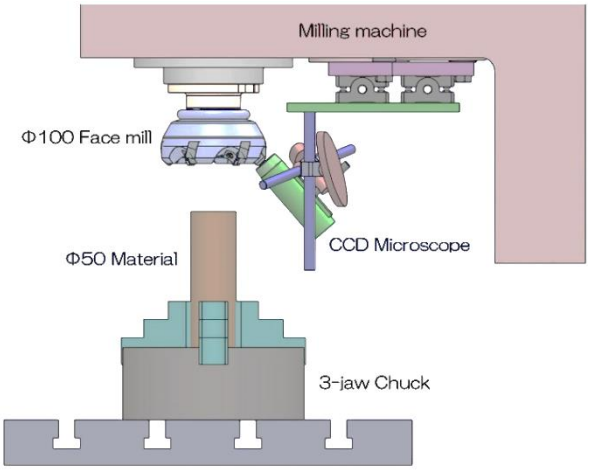

Fig. 4. Experimental set up of tool wear experiment

The cutting distance in one cycle is calculated from the diagram shown in Fig. 5 and Equation (1). The cutting distance in one cycle at each cutting speed is l=16.9 m when V=213 m/min, f=0.12 mm/edge, and l=23.6 m when V=308 m/min, f=0.09 mm/edge. Table 1 summarizes the cutting conditions.

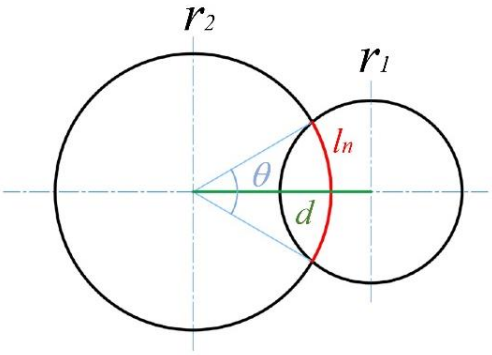

r_1 : Radius of material
r_2 : Radius of face mill
d : The center to center distance between tool and work
l_n : Cutting distance of one revolution

Fig. 5. Geometric diagram of cutting distance.

$$l = \sum_{k=0}^{n-1} \frac{\pi}{180} r_2^2 \cos^{-1}\left\{\frac{\left(r_1 + r_2 - n\bullet f\right)^2 + r_2^2 - r_1^2}{r_1^2 + \left(r_1 + r_2 - n\bullet f\right)^2}\right\} \quad (1)$$

Table 1. Cutting conditions

Condition	200	300
Cutting tool	Φ100 Face mill with One cutting edge	
Cuttig speed (Spindle rotation)	213.5m/min ($680min^{-1}$)	307.9m/min ($980min^{-1}$)
Feed rate (Table feed speed)	0.12mm/edge (81mm/min)	0.09mm/edge (88mm/min)
Depth of cut	1.0mm	
Cutting lubrication	- (Dry cutting)	

The materials used in this experiment were JIS high-toughness steel SCr20 and SCM420. For each material, four work materials were prepared, including forged to annealed material manufactured by the conventional construction method and material forged via SMART forging method. The specifications of the materials are shown in Table 2. For each material, the relationship between the cutting distance and the flank wear width was measured, from the new cutting edge state (flank wear width of 0 mm) to the maximum flank wear width of about 0.6 mm.

Table 2. Specification of the materials (before forging)

JIS		SCr20	SCM420
ISO		20Cr4	- (18CrMO4 ⇕ 34CrMO4)
Chemical composition (%)	Crx100	115	110
	Mo x100	-	18
	Cx100	21	22
	Six100	24	31
	Mnx100	80	78

4. Experimental Results and Discussion

The flank wear width V_B (mm) results from the tool wear experiment are shown in Fig. 6 as a function of the cutting distance l (m). Figure 6-(a) compares the progress of the flank wear width of conventionally forged Cr steel, SMART forged Cr steel, conventionally forged Cr-Mo steel, and the SMART forged Cr-Mo steel at a cutting speed of V=213 m/min. Similarly, Fig. 6-(b) compares the flank wear progress for these four materials, but at a cutting speed of V=308 m/min. In both cases, the progress of initial flank wear is almost identical for all materials. When the state of the tool wear progresses to the steady-state wear region, the progress of the flank wear is slower for the SMART forged material in both Cr and Cr-Mo steel as compared to the conventionally forged materials. This is true for both cutting speeds. Therefore, it is inferred that performing the SMART forging treatment is advantageous in terms of the progress of tool flank wear.

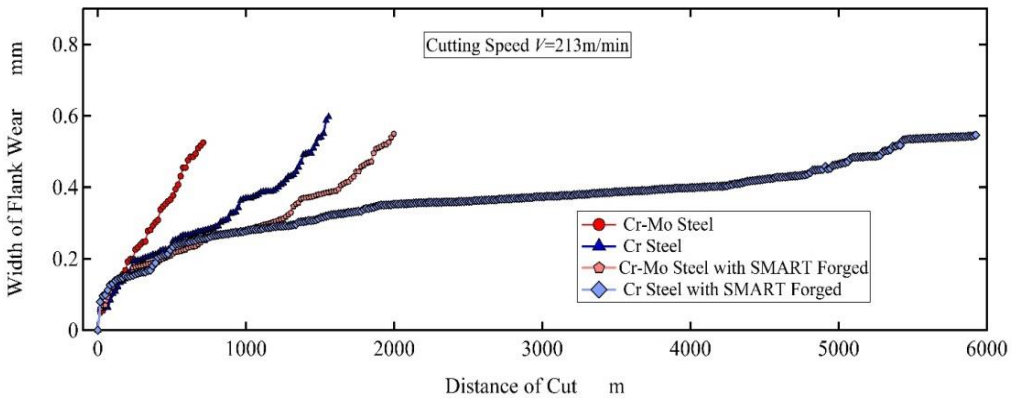

(a) Cutting speed of V=213m/min

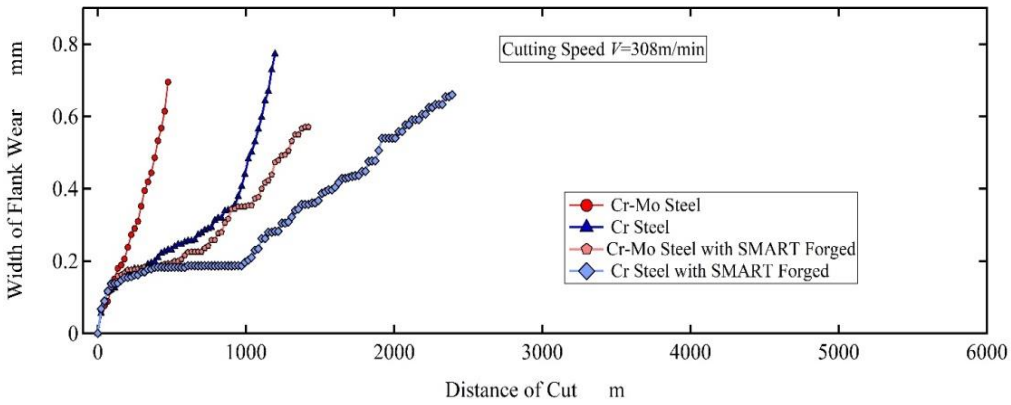

(b) Cutting speed of V=308 m/min

Fig. 6. Relationship between distance of cut and width of flank wear.

4.1. A The Effect of Hardness

The hardness of the materials was measured by the Brinell hardness test because each of the experimental workpieces were forged products. The end faces of each material were polished with a surface-grinding machine. After grinding, the hardness was measured ten times. The average of 8 measurements (excluding the maximum and minimum values) was recorded as the hardness of the material. The results are shown in Fig. 7. It can be seen that there is little variation in the hardness the four materials. Therefore, we conclude that the differences in progression of the flank wear were not due to differences in the hardness of the materials.

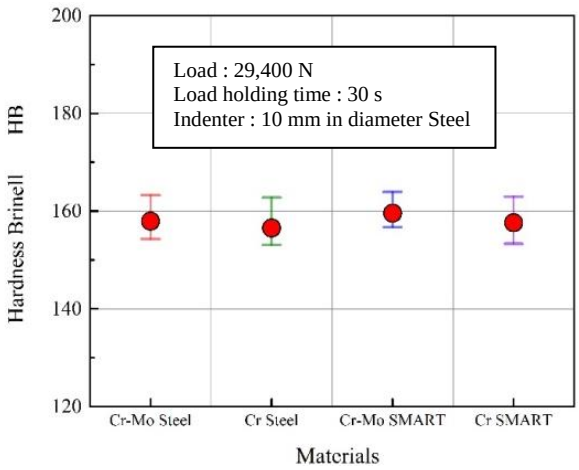

Fig. 7. Brinell hardness of each material.

4.2. The Effect of Grain Size

We suspected that differences in grain size of each material structure might have effects on the progress of frank wear. That is, similarly to sandpaper, if the grain size of the structure is larger, the progress of tool wear will be faster. The photographs in Fig. 8 show the structure of the conventional forged material and the SMART forged material in the Cr-Mo steel. The grain size in the conventionally forged product is clearly smaller. Thus, the difference in progress of the flank wear is not due to the smaller of the grain size. We propose that the progress of flank wear is due to different ratios of constituent ferrite and pearlite. We suspect that forgiveness of tool flank wear has progressed faster due to the larger percentage of pearlite in

conventionally forged materials. In our future work, we will measure the ferrite/perlite ratio in the structure of each material to continue studying this possible dependency.

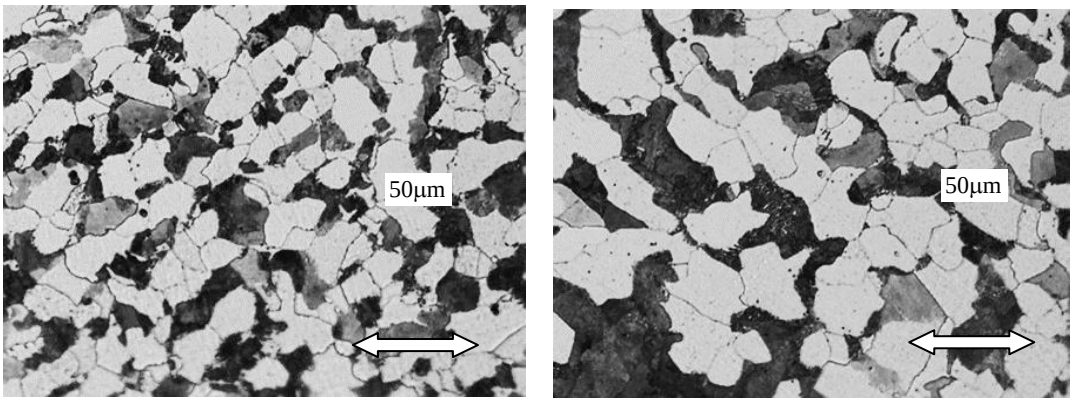

(a) Conventional forged material (b) SMART forged material

Fig. 8. Photograph of the material texture of Cr-Mo steel

4.3. The Effect of Cutting Temperature

Finally, the effect of temperature during the cutting of each material was investigated. The tool-work thermo-electromotive force was measured to determine cutting temperature [3]-[6]. Fig. 9 illustrates the experimental setup. In this portion of the experiment, the investigated cutting speeds were V=409 m/min, V=213 m/min, and V=308 m/min. The feed rates of one cutting edge f were f=0.12 mm/edge (V=213 m/min), f=0.09 mm/edge (V=308 m/min), f=0.12 mm/edge (V=409 m/min). In all cases, the depth of cut t was t=1.0 mm. The same cutting tool described in Section A was used in this test, 100 mm diameter face mill with only one cutting edge attached. Fig. 10 shows the thermo-electromotive force waveform obtained by the cutting experiment. Fig. 10-(a) shows an arbitrary section from the start to the end of cutting, and Fig. 10-(b) shows an enlarged view of one of the sections. The same thermos-electromotive force waveform could be obtained under all the conditions.

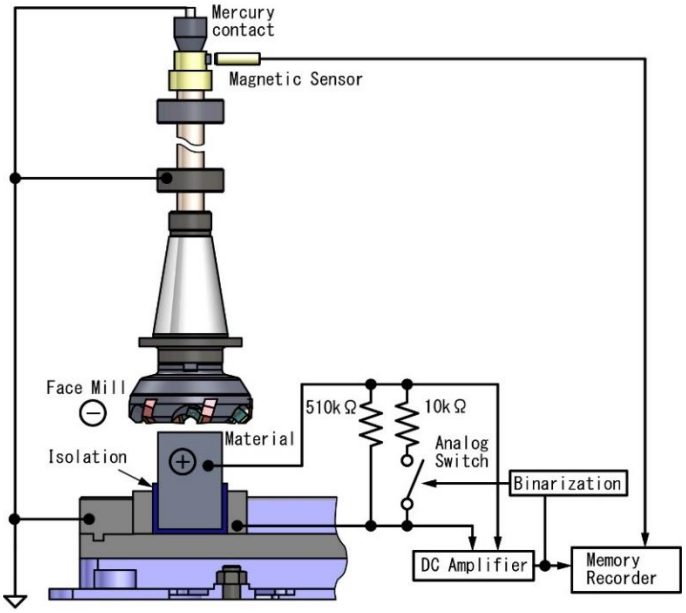

Fig. 9. Experimental set up of tool -work thermos-electromotive force.

In this experiment, we measured the cutting heat generated when each workpiece was cut. The digitalization was performed by using least squares to approximate the portion of the signal when the DC component of thermo-electromotive force was stabilized between the rising edge and the falling edge, and finding the average. A procedure is shown in Fig. 10-(b) and is summarized below.

1. First, data for analysis were created by isolating the DC component of one thermo-electromotive force waveform. Further, 20% of the rising edge of the waveform and 10% before the falling edge, shown in the green regions of Fig. 10-(b), are removed from the cutting time. The time from the rising edge of the thermo-electromotive force to the falling edge are preserved.
2. The data are processed using a least squares approximation of the linear function; see Figure 10-(b).
3. The time corresponding to the middle of the waveform is passed to the function obtained in step 2. The result is assumed to be the average voltage of the waveform, illustrated as the circled point in Fig. 10-(b).
4. For each experimental condition, the process defined in steps 1-3 above are performed for each of the three waveforms. The average value is assumed as the thermo-electromotive force value for each experimental condition.

The results for the measurements described above are shown in Fig. 11. For the scope of this paper, it was sufficient to compare the cutting temperature when cutting each material, so the conversion of thermo-electromotive force to temperature is not necessary.

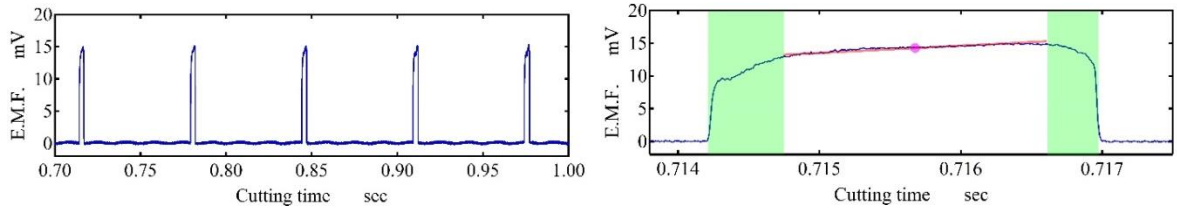

(a) waveform of five cutting cycle (b) Enlarge view of (a) and digitalization procedure

Fig. 10. Waveform of tool-work thermos-electromotive force

In the case of Cr-Mo steel, the cutting temperature was the same for both conventionally forged material and SMART forged material, as shown in Fig. 11. However, for Cr steel, the cutting temperature was lower in the material manufactured via SMART forging. This property became conspicuous when the cutting speed increased. However, the cutting temperature was almost equal for both materials at a cutting speed of V=213 m/min. From these results, we conclude that the progress of tool flank wear of each forged material is not a function of differences in cutting temperature.

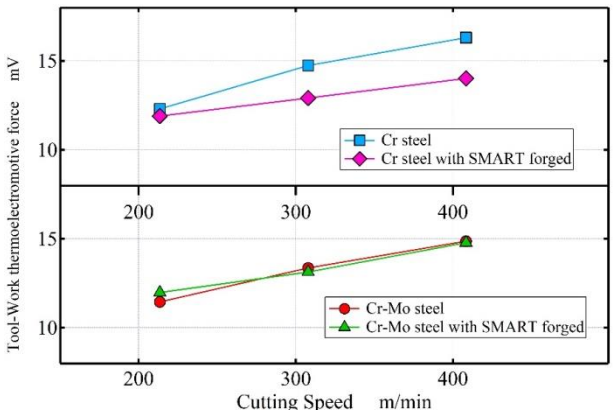

Fig. 11. Relationship between cutting speed and E.M.F in different material.

5. Conclusion

Cr and Cr-Mo steel are high toughness materials, but will have different properties depending on the forging method use. This experiment showed that the progress of the flank wear width of the SMART forged material was slower than materials produced via conventional forging. SMART forged materials were found to be superior in cutting for high speed cutting areas exceeding a cutting speed V=200 m/min.

We first considered if differences in flank wear progress were attributable to material hardness. We completed Brinell tests for the conventionally forged and the SMART forged materials. Results show that there is no noticeable difference in hardness. Therefore, we conclude that differences in the progress of flank wear are not a function of material harness.

In studying effects of the cutting temperature, we find that there was a remarkable difference in the high cutting speed region of Cr steel. However, there was no difference for cutting speed of V=213 m/min. Therefore, we conclude the progress of flank wear is not dependent on cutting temperatures.

We suspect the cause of differences in progress of flank wear is varying ferrite/perlite ratios in the structure of each material. Future work will include studying if and how this feature of the material is cause for changes in flank wear progress.

Acknowledgment

I am thankful to **Kawakami Ironworks Co., Ltd.**, Okayama, Japan, who provided materials for the performance of this experiment. (http://www.kawakami-ironworks.com/)

References

[1] Uchida, K., Hino, M., *et al.* (2017). Material control technology for gear shaft forged products with TMCP (smart forging process). *Journal of JFA,* 58, 77-86.

[2] Uchida, K., Hino, M., *et al.* (2017). Material control technology for gear shaft forged products with TMCP (smart forging process). *Journal of JFA, 59*, 114-126.

[3] Murata, M., Kurokawa, S., Ohnishi, O., Doi, T., & Uneda, M. (2011). Characteristics of thermo-electromotive force, electric current and electric resistance in intermittent cutting process by face milling. *Advanced Materials Research, 314-316*, 1075-1078.

[4] Murata, M., Kurokawa, S., Ohnishi, O., Uneda, M., & Doi, T. (2012). Real-time evaluation of tool flank wear by in-process contact resistance measurement in face milling. *Journal of Advanced Mechanical Design, Systems, and Manufacturing, 6(6)*, 958-970.

[5] Hirota, H., Suzuki, S., & Shinozaki, N. (1979). The correlation between chip breaking and tool-work thermo-electromotive. *Journal of the Japan Society for Precision Engineering, 45(8)*, 39-45.

[6] Hirota, H., Suzuki, S., & Shinozaki, N. (1979). Fluctuating characteristics of tool-work thermo-electromotive force. *Journal of the Japan Society for Precision Engineering, 45(5)*, 68-74.

Mitsuaki Murata was born in Hagi, Yamaguchi, Japan, in 1970. He received the B.S. in engineering degree in 1993 and M.S. in engineering degree in 1995 in Institute of Vocational Training, Japan. He received his Doctor degree in engineering in 2015 in Kyushu University, Japan. Currently he is working as lecturer in Kyushu Sangyo University. His research interest is in-process detection of cutting tool wear.